

## Article

# Calculation and Experimental Verification of Zn–Al–Mg Phase Diagram

Zhao Li <sup>1,2</sup>, Yuanpeng Li <sup>1</sup>, Sheming Jiang <sup>1,\*</sup>, Jie Zhang <sup>1</sup>, Xin Liu <sup>1</sup>, Qifu Zhang <sup>1</sup> and Qiuyuan Liu <sup>1</sup>

<sup>1</sup> National Engineering Laboratory of Advanced Coating Technology for Metals, Central Iron & Steel Research Institute, Beijing 100081, China; 15332811094@163.com (Z.L.); liyuanp9999@163.com (Y.L.); zhangj0212@163.com (J.Z.); lxv20032003@163.com (X.L.); zhqifu@vip.sina.com (Q.Z.); lqydt2011@163.com (Q.L.)

<sup>2</sup> The Technical Center of Bao Gang Group, Baotou 014010, China

\* Correspondence: jiangsheming@263.net

**Abstract:** The liquid phase projection diagram, three-dimensional phase diagram, and vertical section diagram of the Zn–*x*%Al–*x*%Mg alloy system was calculated using the phase diagram calculation software Pandat. Simultaneously making full use of the self-developed hot-dip galvanizing process simulation machine by China Steel Research produced a 75%Zn–19%Al–6%Mg coating. A method combining phase diagram calculations and experimental verification was used to investigate the equilibrium phases and solidification process of the alloy. The microstructure of the 75%Zn–19%Al–6%Mg coating was studied using scanning electron microscopy and energy dispersive spectrometry. The results indicate that the coating structure consists of primary Al dendrite phase, MgZn<sub>2</sub> inter-metallic compound and Zn-rich phase. There is no ternary eutectic structure in the coating structure. Al dendrites grow on the surface of the coating, while there are no Al dendrites on the cross-section. The experimental results strongly concur with the calculated results from the Pandat phase diagram. The solidification sequence of the 75%Zn–19%Al–6%Mg coating is L→L + Al→L + Al + MgZn<sub>2</sub>→Al + MgZn<sub>2</sub> + Zn. The phase diagram guides industrial production significantly, avoiding the waste of transitional materials and zinc caused by small scale trial and error experiments, thus reducing unnecessary production costs. The factory can select a reasonable coating composition designing scheme in the phase diagram, based on the performance requirements of customers for the coating.

**Keywords:** the software of Pandat; phase diagram calculation; 75%Zn–19%Al–6%Mg coating; Zn–Al–Mg alloy microstructure



**Citation:** Li, Z.; Li, Y.; Jiang, S.; Zhang, J.; Liu, X.; Zhang, Q.; Liu, Q. Calculation and Experimental Verification of Zn–Al–Mg Phase Diagram. *Coatings* **2024**, *14*, 468. <https://doi.org/10.3390/coatings14040468>

Academic Editors: Angel Morales Ramirez, Margarita García-Hernández and Aristeo Garrido-Hernández

Received: 23 March 2024  
Revised: 2 April 2024  
Accepted: 10 April 2024  
Published: 12 April 2024



**Copyright:** © 2024 by the authors. Licensee MDPI, Basel, Switzerland. This article is an open access article distributed under the terms and conditions of the Creative Commons Attribution (CC BY) license (<https://creativecommons.org/licenses/by/4.0/>).

## 1. Introduction

Under the effective promotion of national policies, the continuous hot-dip galvanizing industry of strip steel in China has made significant progress in both quantity expansion and quality enhancement after more than 40 years of development. In recent years, with the changes in the international and domestic economic situation, especially the structural transformation of China's steel and related industries, the hot-dip galvanizing industry of strip steel is also facing new challenges [1]. In order to achieve a coating with good comprehensive properties such as plain surface corrosion resistance and a sacrificial corrosion protection ability, zinc-based coatings with different Mg and Al contents have been widely used in the market. Compared to hot-dip galvanized steel and electroplated steel, these coatings exhibit better corrosion resistance in salt spray and cyclic accelerated corrosion tests [2–7]. However, there are currently few articles that explain the solidification process of zinc–aluminum–magnesium coatings based on phase diagrams.

As is well known, the solidification microstructure is a crucial foundational stage in the material preparation and shaping process, typically directly determining the final performance and service life of the material. This paper conducted an in-depth study on the phase transformation rules and properties of the solidification process of Zn-based coatings

with different Mg and Al contents using the Pandat software produced by the American company Compu-Therm LLC (Middleton, WI, USA), providing theoretical support for industrial production. In the current market, there are Zn–Al–Mg alloy coatings with an Al content not exceeding 11.0% and a Mg content not exceeding 3.0%. Few scholars have studied Zn–Al–Mg coatings with high Al and Mg content. This article combines simulation calculations with laboratory verification to successfully predict and confirm the solidification structure and process of 75%Zn–19%Al–6%Mg alloy coating, laying the foundation for the subsequent development of this coating formula.

## 2. Pandat

### 2.1. Pandat Basics

Pandat [8] is a software package for multi-component phase diagram calculation and materials property simulation, developed by the American company Compu-Therm LLC. Pandat software is an integrated computational tool developed based on the CALPHAD (calculation of phase diagram) approach. It has a robust thermodynamic calculation engine, a friendly graphical user interface, and a flexible post-calculation table editing function which allows the user to plot various types of diagrams. The software is designed to create a working environment that allows a variety of calculation modules to be integrated in the same workspace. The architecture of Pandat software is schematically shown in Figure 1.

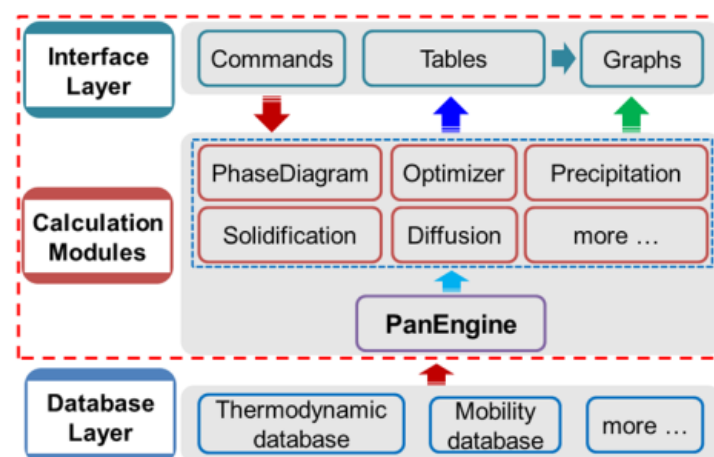


**Figure 1.** The architecture of Pandat software.

### 2.2. Establishment of Thermodynamic Model

The thermodynamic model is the prerequisite to fulfill the phase diagram and thermodynamic property calculation. A thermodynamic database represents a set of self-consistent Gibbs-energy functions with optimized thermodynamic model parameters for all the phases in a system. The advantage of the CALPHAD method is that the separately measured phase diagrams and thermodynamic properties can be represented by a unique “thermodynamic description” of the materials system in question. More importantly, based on the known descriptions of the constituent lower-order systems, the thermodynamic description for a higher-order system can be obtained via an extrapolation method [9]. This description enables us to calculate phase diagrams and thermodynamic properties of multi-component systems that are experimentally unavailable.

Thermodynamic models used to describe the disordered phase, ordered inter-metallic phase and stoichiometric phase are presented. The equations are given for a binary system, and they can be extrapolated to a multi-component system using geometric models [9,10].

The Gibbs energy of a binary (such as Al and Zn) disordered solution phase can be written as:

$$G_m^\phi = \sum_{i=Zn,Al} x_i G_i^{\phi,0} + RT \sum_{i=Zn,Al} x_i \ln x_i + x_{Zn} x_{Al} \sum_v L_v (x_{Zn} - x_{Al})^v \quad (1)$$

Here,  $\sum_{i=Zn,Al} x_i G_i^{\phi,0}$  are the reference states.  $RT \sum_{i=Zn,Al} x_i \ln x_i$  is the entropy of ideal mixing.  $x_{Zn} x_{Al} \sum_{\nu} L_{\nu} (x_{Zn} - x_{Al})^{\nu}$  is the excess Gibbs energy of mixing.  $x_i$  is the mole fraction of a component  $i$ ,  $G_i^{\phi,0}$  is the Gibbs energy of pure component  $i$ , with  $\phi$  structure,  $R$  is the gas constant,  $T$  is the absolute temperature,  $L_{\nu}$  is the interaction coefficient in the polynomial series of the power  $\nu$ . Equation (1) can be interpolated into a multi-component system using geometric models [10].

For a Zn–Al multi-component solution phase with Mg components, the following equation is used:

$$G^{\phi} = \sum_{i=Zn,Al,Mg}^c x_i G_i^{\phi,0} + RT \sum_{i=Zn,Al,Mg}^c x_i \ln x_i + E_{G^{bin,\phi}} + E_{G^{tern,\phi}} + \dots \quad (2)$$

The excess contributions are:

$$E_{G^{bin,\phi}} = \sum_{i=1}^{c-1} \sum_{j>i}^c x_i x_j \sum_{\nu=0}^n L_{ij}^{\nu,\phi} (x_i - x_j)^{\nu} \quad (3)$$

$$E_{G^{tern,\phi}} = \sum_{i=1}^{c-2} \sum_{j>i}^{c-1} \sum_{k>j}^c x_{Zn} x_{Al} x_{Mg} \{ L_{ZnAlMg}^{0,\phi} (x_{Zn} + \delta_{ZnAlMg}) + L_{ZnAlMg}^{1,\phi} (x_{Zn} + \delta_{ZnAlMg}) + L_{ZnAlMg}^{2,\phi} (x_{Zn} + \delta_{ZnAlMg}) \} \quad (4)$$

$$\delta_{ZnAlMg} = (1 - x_{Zn} - x_{Al} - x_{Mg})/3 \quad (5)$$

For ternary systems,  $x_{Zn} + x_{Al} + x_{Mg} = 1$ ,  $\delta_{ZnAlMg} = 0$ . In a ternary system, if all the three  $L$  parameters are identical,

$$L_{ZnAlMg}^{0,\phi} = L_{ZnAlMg}^{1,\phi} = L_{ZnAlMg}^{2,\phi} = L_{ZnAlMg}^{\phi} \quad (6)$$

then

$$E_{G^{tern,\phi}} = \sum_{i=1}^{c-2} \sum_{j>i}^{c-1} \sum_{k>j}^c x_{Zn} x_{Al} x_{Mg} L_{ZnAlMg}^{\phi} \quad (7)$$

In Panda, if only one ternary interaction parameter  $L_{ZnAlMg}^{0,\phi}$  is provided, Panda will treat three ternary interaction parameters as the symmetrical case, i.e., all three parameters have the same value.

An ordered inter-metallic phase is described by a variety of sub-lattice models, such as the compound energy formalism [11,12] and the bond energy model [13,14]. In these models, the Gibbs energy is a function of the sub-lattice species concentrations and temperature. The molar Gibbs energy of a binary inter-metallic phase, described by a two-sub-lattice compound energy formalism,  $(A, B)_p:(A, B)_q$ , can be written as:

$$G_m^{\phi} = \sum_{Zn=A,B} \sum_{j=A,B} y_{Zn}^I y_{Mg}^{II} G_{Zn:Mg}^{\phi} + RT \left( \frac{p}{p+q} \sum_{Zn=A,B} y_{Zn}^I \ln y_{Zn}^I + \frac{q}{p+q} \sum_{Zn=A,B} y_{Zn}^{II} \ln y_{Zn}^{II} \right) + \sum_{Mg=A,B} y_A^I y_B^I y_{Mg}^{II} \sum_{\nu} (y_A^I - y_B^I)^{\nu} L_{A,B:Mg}^{\nu} + \sum_{Zn=A,B} y_{Zn}^I y_A^{II} y_B^{II} \sum_{\nu} (y_A^{II} - y_B^{II})^{\nu} L_{Zn:A,B}^{\nu} + y_A^I y_B^I y_A^{II} y_B^{II} L_{A,B:A,B} \quad (8)$$

where  $y_{Zn}^I$  and  $y_{Zn}^{II}$  are the species concentrations of a component Zn, in the first and second sub-lattices, respectively. The first term on the right hand of the equation represents the reference state with the mechanical mixture of the stable or hypothetical compounds:  $A_{p+q}$ ,  $A_p B_q$ ,  $B_p A_q$  and  $B_{p+q}$ .  $G_{Zn,Mg}^{\phi}$  is the Gibbs energy of the stoichiometric compound,  $Zn_p Mg_q$  with a  $\phi$  structure. Sometimes,  $G_{Zn,Mg}^{\phi}$  is treated as model parameters to be obtained through optimization using the experimental data related to this phase. The second term is the ideal mixing Gibbs energy, which corresponds to the random mixing of species on the first and second sub-lattices. The last three terms are the excess Gibbs energies of mixing.

The  $L$  parameters in these terms are model parameters whose values are obtained using the experimental phase equilibrium data and thermodynamic property data. These parameters can be temperature dependent. In this equation, a comma is used to separate species in the same sub-lattice, whilst a colon is used to separate species belonging to different sub-lattices. The compound energy formalism can be applied to phases in a multi-component system by considering the interactions from all the constituent binaries. Additional ternary and higher-order interaction terms may also be added to the excess Gibbs energy term.

### 2.3. Zn–Al–Mg Thermodynamic Parameters

Table 1 provides detailed thermodynamic parameters for zinc, aluminum, and magnesium elements. The element aluminum, the chemical symbol Al, has a face-centered cubic crystal structure. The element magnesium, the chemical symbol Mg, has a hexagonal close-packed crystal structure. The element zinc, chemical symbol Zn, has a hexagonal close-packed crystal structure.  $H_{298}$  and  $S_{298}$ , respectively, refer to enthalpy and entropy values at a temperature of 298 K.

**Table 1.** Thermodynamic parameters.

Name	Structure	Atomic Number	Atomic Weight/g	$H_{298}$ /J/mol	$S_{298}$ /J/K·mol
Al	Fcc	13	26.982	4540	28.300
Mg	Hcp	12	24.305	4998	32.671
Zn	Hcp	30	65.390	5657	41.630

## 3. Phase Diagram Calculation

### 3.1. Ternary Phase Diagram and Liquidus Surface Projection of the Zn–Al–Mg System

Currently, mature zinc–aluminum–magnesium coatings available on the market and zinc–aluminum–magnesium coatings studied in the laboratory have an Al element content of no more than 25% and an Mg element content of no more than 15%. However, to clearly label the actual composition points or ranges of the research coatings in the liquidus surface projection diagram, this article used the Pandat software to draw the ternary phase diagram of Zn–Al–Mg, setting the Al and Mg contents to not exceed 30%.

Figure 2a is the three-dimensional diagram of the Zn–Al–Mg coating ternary phase diagram, and Figure 2b is its liquidus surface projection diagram. From Figure 2b, the following results can be produced.

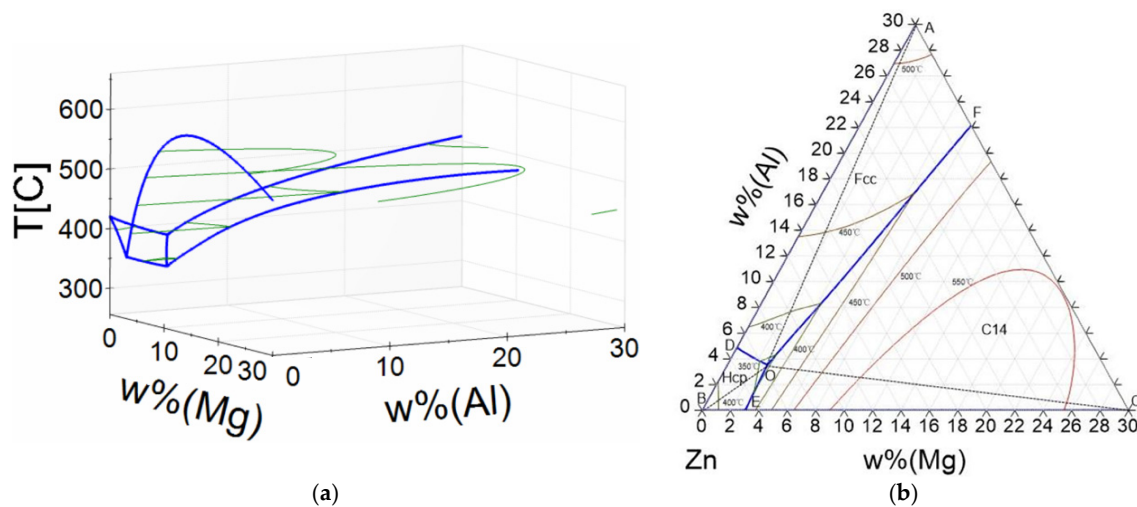


**Figure 2.** Three-dimensional phase diagram of Zn–Al–Mg and liquid surface projection diagram: (a) Zn–Al–Mg 3D phase diagram; (b) liquid surface projection diagram.

The quadrilateral region “AFOD” represents the single-phase Al region with a face-centered cubic crystal structure (Fcc).

The quadrilateral region “FOEC” represents the single-phase region of the Laves\_C14 inter-metallic compound  $\text{MgZn}_2$ .

The quadrilateral region “OEBD” represents the single-phase Zn region with a hexagonal close-packed crystal structure (Hcp).

The “OD” line is the eutectic line between the Fcc\_Al phase and the Hcp\_Zn phase.

The “OF” line is the eutectic line between the Fcc\_Al phase and the Laves\_C14\_MgZn<sub>2</sub> phase.

The “OE” line is the eutectic line between the Hcp\_Zn phase and the Laves\_C14\_MgZn<sub>2</sub> phase.

The point “O” represents the ternary eutectic region of the final solidification of the Fcc\_Al phase, Hcp\_Zn phase, and Laves\_C14\_MgZn<sub>2</sub> phase.

The “OA” line is the solidification line of the single-phase Fcc\_Al.

The “OC” line is the solidification line of the single-phase Laves\_C14\_MgZn<sub>2</sub> inter-metallic compound.

The “OB” line is the solidification line of the single-phase Hcp\_Zn.

Furthermore, we can also deduce from the isothermal lines in the liquidus surface projection diagram of the Zn–Al–Mg ternary phase diagram that as the content of Al and Mg alloy elements increases, the melting point of the coating rises. At point B, the Zn content is 100%, and the temperature of the isothermal line is 400 °C. Increasing the concentration of Al along the “BA” line, the temperature of the isothermal line rises to 500 °C. Increasing the concentration of Mg, which is the same as Al, along the “BC” line from point B, the highest temperature of the isothermal line rises to 550 °C.

This phase diagram guides industrial production significantly, avoiding the waste of transitional materials and zinc caused by small-scale trial and error experiments, thus reducing unnecessary production costs. The factory can choose a reasonable coating composition design scheme in the phase diagram based on the specific performance requirements of the coating from the final customers. For example, we can choose to design the coating composition in the quadrilateral region “AFOD” to solidify along the diagonal line “AO”. From the isothermal curves in the diagram, it can be seen that as the temperature decreases from 500 °C, solidification gradually occurs, passing through 450 °C and 400 °C, until reaching 350 °C, finally solidifying into a ternary eutectic structure. By designing such a composition, the final solidified structure of the coating consists of an initially precipitated Al-rich phase followed by the final solidification of the Zn–Al–MgZn<sub>2</sub> ternary eutectic structure. This effectively avoids the binary eutectic regions along the “OF” and “OD” lines, resulting in a significant improvement in the surface color difference of the product. Similarly, we can also choose to avoid the brittle Zn–Al–MgZn<sub>2</sub> ternary eutectic structure and produce a manufacturing structure consisting of either Al-rich phase + Al–MgZn<sub>2</sub> binary eutectic structure or Al-rich phase + Zn–Al binary eutectic structure. The galvanizing factory can choose the appropriate production scheme according to its actual situation. This article will not list them one by one.

### 3.2. Zn-19%Al-x%Mg Vertical Section

Figure 3 is a vertical section of the three-dimensional phase diagram of Zn–19%Al–x%Mg. The method used to generate Figure 3 was to fix the mass percentage of the Al element concentration at 19%, with the horizontal axis representing the concentration of the Mg element and the vertical axis representing temperature.

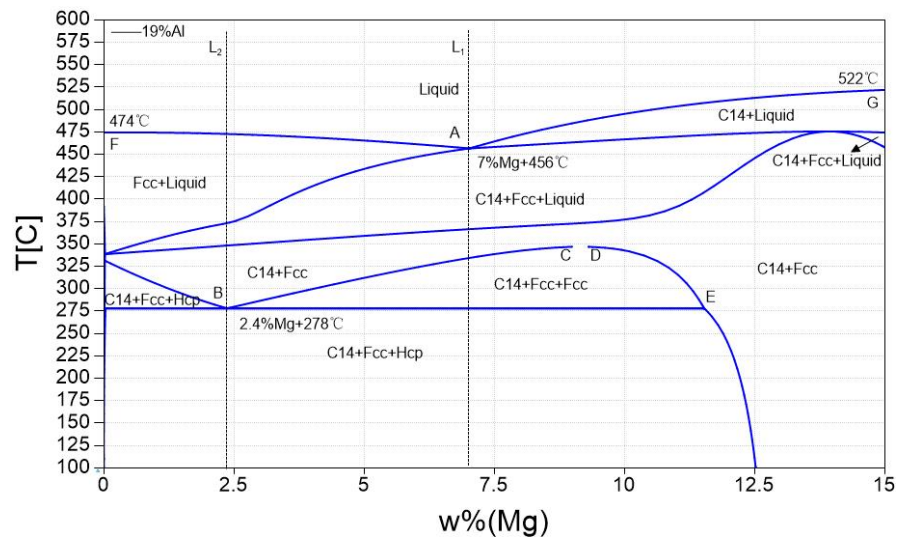


Figure 3. Vertical section of Zn–19%Al– $x$ %Mg phase diagram.

Given the complexity of the Zn–Al–Mg alloy phase diagram, this article just selected specific individual points for analysis. Point A is a eutectic point in the solidification process of the Zn–19%Al– $x$ %Mg ternary alloy. When the Mg content is 7%, the liquidus temperature of Zn–19%Al–7%Mg decreases to 456 °C, meanwhile, both the face-centered cubic (Fcc) Al phase and the Laves\_C14 phase MgZn<sub>2</sub> inter-metallic compound precipitate from the liquid phase. A vertical line, L1, is drawn on the horizontal axis at the point with 7% Mg content, which represents the Mg content line at the eutectic position of Zn–19%Al–7%Mg.



When the Mg content is less than 7%, as the temperature decreases, the liquid Zn–19%Al– $x$ %Mg phase will first precipitate the Al-rich phase along the FA line. The point F, with 0% Mg content, starts to precipitate at a temperature of 474 °C.

When the Mg content is greater than 7%, as the temperature decreases, the liquid Zn–19%Al– $x$ %Mg phase will first precipitate the Laves\_C14 phase MgZn<sub>2</sub> inter-metallic compound along the GA line. The point G, with 15% Mg content, starts to precipitate at a temperature of 522 °C. This phenomenon once again confirms that with the increase in Mg content, the melting point of the Zn–Al–Mg alloy increases. As the Mg content increases from 0% to 15%, the melting point of the plating solution increases by 48 °C.

Point B is a eutectic point in the solidification process of the Zn–19%Al– $x$ %Mg ternary alloy. When the Mg content is 2.4%, the temperature of the Zn–19%Al– $x$ %Mg solution decreases, and the Al-rich phase first precipitates from the liquid phase. At this point, the coating structure consists of the initially precipitated Al-rich phase and the remaining liquid phase, forming a semi-solidified slurry-like region. As the temperature further decreases, the MgZn<sub>2</sub> phase gradually precipitates in the coating. The coating structure changes to consist of the Al-rich phase and the MgZn<sub>2</sub> phase. Along the L2 line, as the coating temperature continues to decrease to 278 °C, a eutectic reaction occurs in the coating, and the zinc-rich phase that the crystal structure is hexagonal close-packed (Hcp) starts to precipitate.



In the phase diagram, along the BC and DE lines, the Al phase undergoes an allotropic transformation. At high temperatures, the Al phase contains a large amount of dissolved Zn elements. As the temperature decreases, the supersaturated Zn elements precipitate out to form a zinc-rich phase. Due to the difference in the solubility of Zn elements in the two Al phases, the lattice constants of the two Al phases are different.

### 3.3. Zn-x%Al-6%Mg Vertical Section

Figure 4 is a vertical section of the three-dimensional phase diagram of Zn-x%Al-6%Mg. The method used to plot Figure 4 is similar to that of Figure 3, with the fixed mass percentage of Mg element at 6%. The horizontal axis represents the concentration of the Al element, and the vertical axis represents temperature. For the Zn-x%Al-6%Mg phase diagram in Figure 4, this study focuses on three typical equilibrium phase transition points labeled as C, D, and E. For other phenomena, the same analysis method can be used according to actual production needs to conduct analysis and guide production, thereby achieving the expected coating.

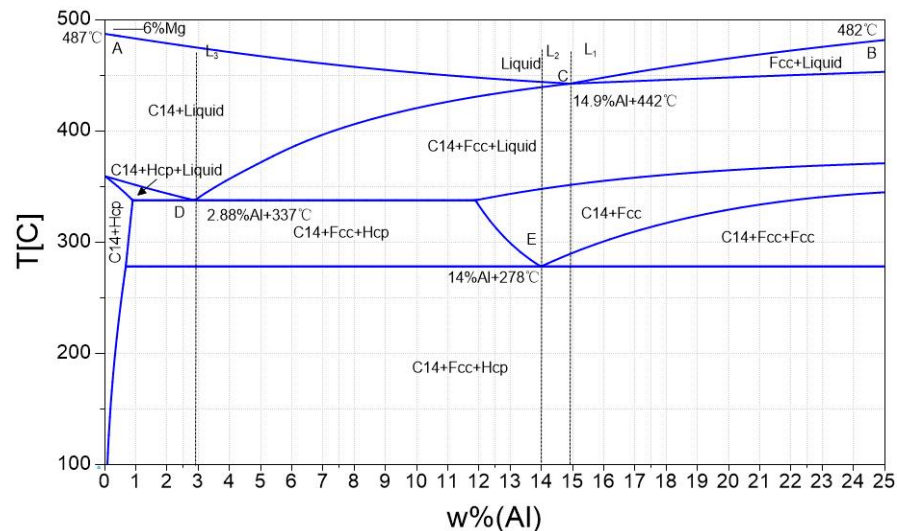


**Figure 4.** Vertical section of Zn-x%Al-6%Mg phase diagram.

Point C is also a eutectic point in the solidification process of the Zn-x%Al-6%Mg ternary alloy. When the Al content is 14.9%, in the Zn-14.9%Al-6%Mg alloy, with the solution temperature decreasing gradually along line L1, the temperature drops to 442 °C. At this point, at both the face-centered cubic (Fcc) Al phase and the Laves\_C14 phase, the MgZn<sub>2</sub> inter-metallic compound precipitates from the liquid phase.



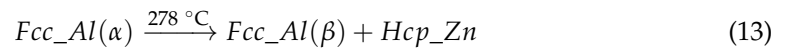
When the Al content is less than 14.9%, with the temperature decreasing at the Laves\_C14 phase, the MgZn<sub>2</sub> inter-metallic compound precipitates from the liquid phase of Zn-x%Al-6%Mg, along line AC. The point A represents that the precipitation temperature is 487 °C when the Al content is 0%.

When the Al content is greater than 14.9%, with the temperature decreasing, the Al-rich phase precipitates from the liquid phase of Zn-x%Al-6%Mg, along line BC. Point B represents that the precipitation temperatures is 482 °C when the Al content is 25%. Comparing the precipitation temperatures of points A and B, it can be concluded that the concentration of Al has little impact on the melting point of the Zn-Al-Mg alloy.

Point D is another eutectic point in the solidification process of the Zn-x%Al-6%Mg ternary alloy. When the Al content is 2.88% (Point D), with the temperature decreasing at the Laves\_C14 phase, the MgZn<sub>2</sub> inter-metallic compound firstly precipitates from the liquid phase of Zn-2.88%Al-6%Mg, along line L3. At this point, the coating structure consists of a semi-solid, pasty region composed of the MgZn<sub>2</sub> phase and residual liquid phase. As the temperature further decreases to 337 °C, the remaining liquid phase undergoes eutectic reaction and precipitates both the Al and Zn phases.



Point E is a eutectic point in the solidification process of the Zn- $x\%$ Al-6%Mg ternary alloy. When the Al content is 14%, with the temperature decreasing during the Laves\_C14 phase, the MgZn<sub>2</sub> inter-metallic compound firstly precipitates from the liquid phase, along line L2. At this point, the coating structure consists of a semi-solid, pasty region composed of the MgZn<sub>2</sub> phase and residual liquid phase. As the temperature further decreases, the Fcc\_Al phase gradually precipitates in the coating, resulting in a structure composed of the Al phase, MgZn<sub>2</sub> phase, and residual liquid phase. When the temperature drops to 278 °C, a eutectic reaction occurs in the coating with the supersaturated Zn element precipitating from the Al phase, with a high amount forming in the Zn-rich phase with a hexagonal close-packed (Hcp) structure.



## 4. Experimental Verification

### 4.1. Experimental Procedure

This article fully utilizes the multi-functional galvanizing process simulation equipment independently developed by the “National Engineering Laboratory for Advanced Metallic Materials Coating” at China Iron and Steel Research Institute (Figure 5). The intermediate alloy ingot was added to the zinc pot, and cold-rolled material DC01 was used for galvanizing to produce the 75%Zn-19%Al-6%Mg coating.

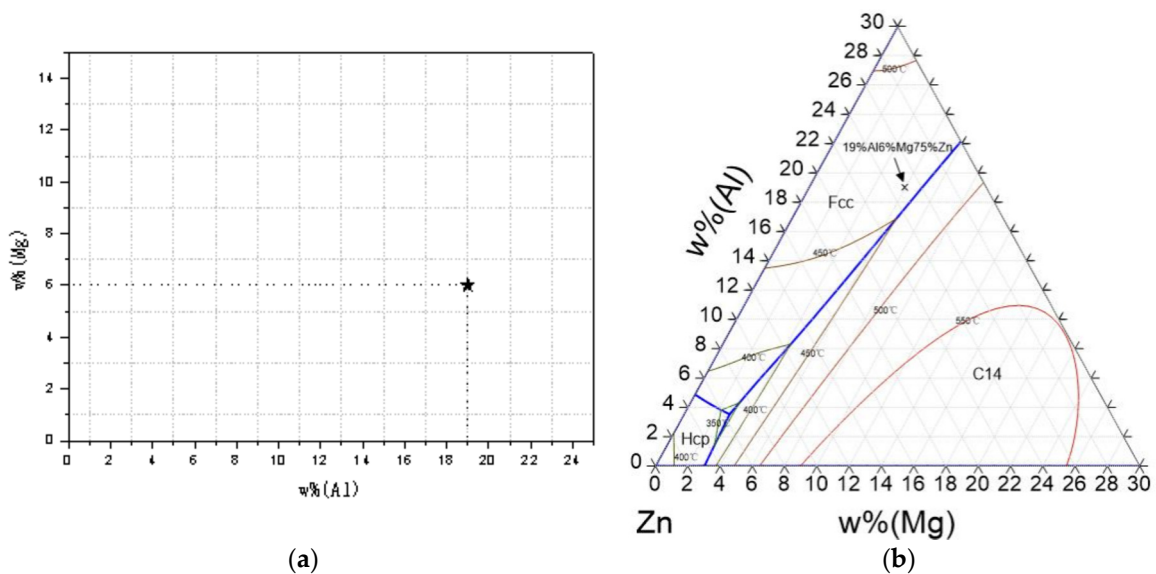


**Figure 5.** CGA-2010 multi-functional galvanizing process simulation equipment.

The 75%Zn-19%Al-6%Mg coating was made into small test samples, and then the surface and cross-section of the coating were analyzed for structure and composition, using scanning electron microscopy, EDS spectroscopy, and a XRD diffract meter.

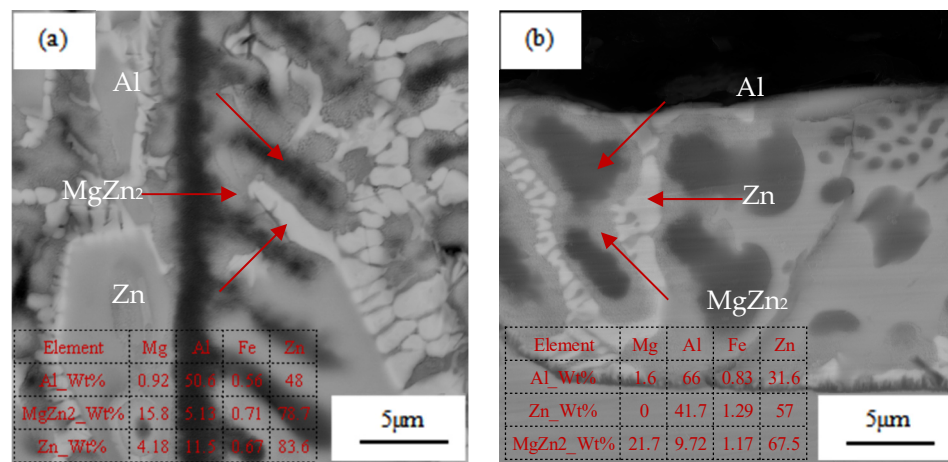
### 4.2. Results and Analysis

Figure 6 shows the comparison between the alloy composition of the 75%Zn-19%Al-6%Mg coating in the laboratory experiment and the liquid surface projection of the ternary phase diagram. In this article, the Zn-Al-Mg coating involves adding 19% of Al elements by mass and 6% of Mg elements by mass to the zinc-based coating.



**Figure 6.** Laboratory-produced 75%Zn-19%Al-6%Mg coating alloy composition and liquid surface projection diagram: (a) the mass fraction of component; (b) liquid phase projection diagram.

Here, an example of an SEM backscattered electron image of the 75%Zn19%Al6%Mg alloy layer at a polished surface and polished cross-section that refers to the direction perpendicular to the surface is shown in Figure 7a,b. Figure 7 is an SEM backscattered electron image at a magnification of 5000×.



**Figure 7.** The microstructure of the 75%Zn-19%Al-6%Mg coating: (a) the surface structure of the coating; (b) the cross-section of the coating.

In the SEM backscattered electron image, three values that are defined as the lightness of the grayscale, the hue, and the contrast that are expressed by each phase in the Zn-Al-Mg alloy layer are determined. Since the three values, that are the lightness, hue, and contrast that is exhibited by each phase, reflect the atomic number of the element included in each phase, usually, there is a tendency for phases that contain higher contents of Al or Mg that have small atomic numbers to exhibit a black color, and phases that contain higher contents of Zn to exhibit a white color.

Note that, in Figure 7a,b, Al indicates the Al crystals, Zn indicates the Zn phase, and MgZn<sub>2</sub> indicates the MgZn<sub>2</sub> phase.

The structure of the 75%Zn-19%Al-6%Mg coating designed in this article consists of the primary Al dendrite phase + MgZn<sub>2</sub> inter-metallic compound + Zn-rich phase [15,16]. There is no ternary eutectic structure in the structure of the 75%Zn-19%Al-6%Mg coating.

The Al dendrites grow on the surface of the coating, while there are no Al dendrites on the cross-section.

The X-ray diffraction (XRD) pattern of the 75%Zn–19%Al–6%Mg coating sample produced in the laboratory experiment is shown in Figure 8, using a Cu-K $\alpha$  ray. From the data in Figure 8, it can be seen that the structure of the experimentally produced coating consists of the Al phase + MgZn<sub>2</sub> inter-metallic compound + Zn phase, which is consistent with the predicted results from the phase diagram.

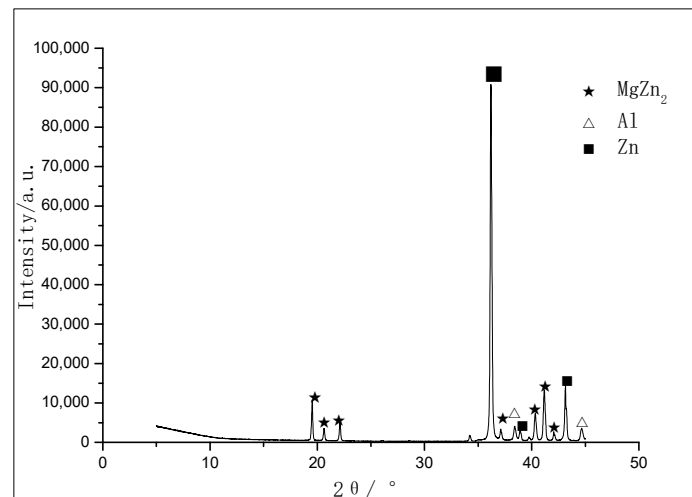


**Figure 8.** XRD image of the 75%Zn–19%Al–6%Mg coating.

Combining Figure 7, the solidification process of the 75%Zn–19%Al–6%Mg coating was carefully analyzed using the Pandat software (as shown in Figure 9a). Figure 9a is based on Figure 4, with a parallel line L drawn at the 19% position on the  $x$ -axis. Along line BC, the Fcc\_Al dendrite phase firstly precipitates from the liquid phase in the AB segment, with the temperature of 75%Zn19%Al6%Mg alloy decreasing. Continuing to decrease the temperature of the alloy layer, the C14\_MgZn<sub>2</sub> inter-metallic compound precipitates in the coating in the BC segment, with the coating structure consisting of the liquid phase, Al phase, and MgZn<sub>2</sub>. In the CD segment, the coating structure is the Al phase and MgZn<sub>2</sub> inter-metallic compound, with the highest amount of Zn elements dissolved in the Al phase. From the DE segment to room temperature, the phase transformation of eutectic co-precipitation occurs in the coating:  $Fcc\_Al(\alpha) \rightarrow Fcc\_Al(\beta) + Hcp\_Zn$ . The original Al phase transforms into a new Al phase and Zn phase, however, the concentration of dissolved Zn elements in these two Al phases is different. As the temperature decreases, supersaturated Zn elements precipitate from the Al phase to form a Zn-rich phase.

Figure 9b is an SEM backscattered electron image of the 75%Zn–19%Al–6%Mg coating at a magnification of 10,000 $\times$ . Figure 9b is an EDS line analysis spectrum of the Al dendrite phase. Using a scanning electron microscope, a line scan is performed from the center to the edge of the Al phase. Figure 9c shows that the concentration of Zn elements gradually increases from the center to the edge of the Al phase, while the concentration of the Al elements decreases gradually. The actual experimental results are consistent with the predicted results from the phase diagram calculations, demonstrating the feasibility of the phase diagram calculations.

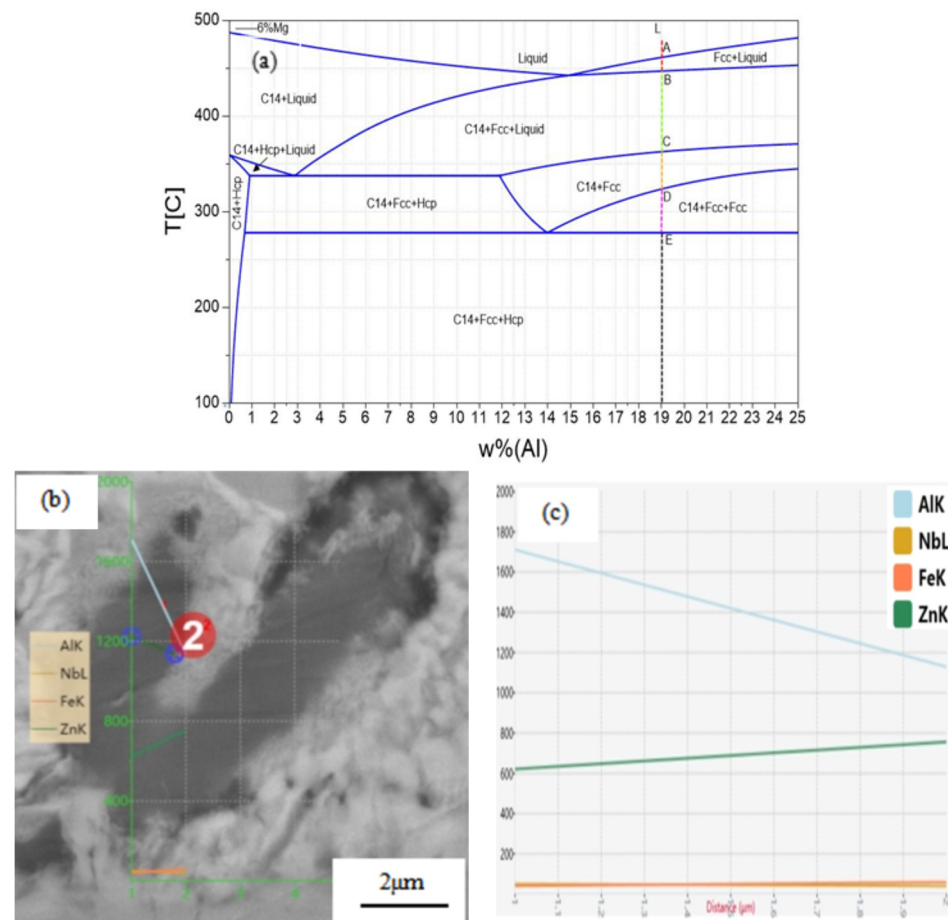


**Figure 9.** Phase diagram and electron line scan results of the 75%Zn–19%Al–6%Mg: (a) 75%Zn–19%Al–6%Mg phase diagram; (b) SEM backscattered electron image of the coating cross-section; (c) EDS line scan image.

## 5. Conclusions

From a comprehensive analysis of the phase diagram calculations and laboratory experimental results of the 75%Zn–19%Al–6%Mg coating, the following conclusions have been drawn.

1. The solidification structure of the 75%Zn–19%Al–6%Mg coating and the solidification process of the alloy calculated by phase diagram software (Pandat) are consistent with the experimental results.
2. This paper used the Pandat software to calculate the ternary phase diagram and composition section of Zn–Al–Mg. The results of the phase diagram calculations can provide theoretical support for laboratory research and large-scale industrial production.
3. In the laboratory, 75%Zn–19%Al–6%Mg coating was produced by the CGA-2010 multifunctional galvanizing process simulation equipment. The solidification structure of this alloy is the primary Al dendrite phase +  $MgZn_2$  intermetallic compound + Zn-rich phase. There is no ternary eutectic structure in the coating microstructure. The Al dendrites grew on the surface of the coating, without the presence of Al dendrites on the cross-section.
4. The phase diagram calculation results show that the solidification sequence of 75%Zn–19%Al–6%Mg is  $L \rightarrow L + Al \rightarrow L + Al + MgZn_2 \rightarrow Al + MgZn_2 + Zn$ . Adding different contents of Al and Mg elements to the Zn-based plating solution changes the melting point of the solution. The element Al contributes little to the melting point of the solution, but with the increase in Mg concentration, the melting point of the solution rises. As the

Mg content increases from 0% to 15%, the melting point of the plating solution increases by 48 °C.

**Author Contributions:** Methodology, Y.L., J.Z., X.L., Q.Z. and Q.L.; Writing—original draft, Z.L.; Writing—review & editing, S.J. All authors have read and agreed to the published version of the manuscript.

**Funding:** This research received no external funding.

**Institutional Review Board Statement:** Not applicable.

**Informed Consent Statement:** Not applicable.

**Data Availability Statement:** Data are contained within the article.

**Conflicts of Interest:** The authors declare no conflict of interest.

## References

1. Gu, T.; Liu, Y.; Peng, C.; Zhang, P.; Wang, Z. The inhibition effect of ultraviolet illumination on a simulated extremely cold atmospheric corrosion for zinc-aluminum-magnesium coating. *J. Mater. Res. Technol.* **2023**, *22*, 3319–3330. [[CrossRef](#)]
2. Koll, T.; Ullrich, K.; Faderl, J.; Hagler, J.; Spalek, A. Properties and Potential Applications of ZnMg Alloy Coatings on steel sheet by PVD. In Proceedings of the Galvatech' 04, 6th International Conference on Zinc and Zinc Alloy Coated Steel, Chicago, IL, USA, 4–7 April 2004.
3. Thierry, D.; Prosek, T.; Le Bozec, N.; Diller, E. Corrosion protection and corrosion mechanisms of continuous galvanised steel sheet with focus on new coatings alloys. In Proceedings of the Galvatech' 11, 8th International Conference on Zinc and Zinc Alloy Coated Steel, Genoa, Italy, 21–25 June 2011.
4. Yu, Z.; Hu, J.; Meng, H. A Review of Recent Developments in Coating Systems for Hot-Dip Galvanized Steel. *Front. Mater.* **2020**, *7*, 74. [[CrossRef](#)]
5. Koch, G.H.; Brongers, M.P.; Thompson, N.G.; Virmani, Y.P.; Payer, J.H. *Corrosion Cost and Preventive Strategies in the United States*; Federal Highway Administration: Washington, DC, USA, 2002.
6. LeBozec, N.; Thierry, D.; Persson, D.; Stoullil, J. Atmospheric Corrosion of Zinc-Aluminum Alloyed Coated Steel in Depleted Carbon Dioxide Environments. *J. Electrochem. Soc.* **2018**, *165*, C343. [[CrossRef](#)]
7. Thierry, D.; Le Bozec, N.; Persson, D. Corrosion of Hot-Dip-Galvanized Steel and Zinc Alloy-Coated Steel in Ammonia and Ammonium Chloride. *Mater. Corros.* **2020**, *71*, 1118–1124. [[CrossRef](#)]
8. Available online: <https://computherm.com/software> (accessed on 21 January 2024).
9. Chou, K.C.; Austin Chang, Y. A study of Ternary Geometrical Models. *Ber. Bunsenges. Phys. Chem.* **1989**, *93*, 735–741. [[CrossRef](#)]
10. Muggianu, Y.M.; Gambino, M.; Bros, J.P. Enthalpies of formation of liquid alloys bismuth-gallium tin at 723K-choice of an analytical representation of integral and partial thermodynamic functions of mixing for this ternary system. *Chim. Phys.* **1975**, *72*, 83–88. [[CrossRef](#)]
11. Ansara, I. Comparison of methods for thermodynamic calculation of phase diagrams. *Int. Metal Rev.* **1979**, *24*, 20–53.
12. Ansara, I.; Sundman, B.; Willemin, P. Thermodynamic modeling of ordered phases in the Ni-Al system. *Acta Metall.* **1988**, *36*, 977–982. [[CrossRef](#)]
13. Oates, W.A.; Wenzl, H. The bond-energy model for ordering in a phase with sites of different coordination numbers. *Calphad* **1992**, *16*, 73–78. [[CrossRef](#)]
14. Chen, S.L.; Kao, C.R.; Chang, Y.A. A generalized quasi-chemical model for ordered multi-component, multi-sub-lattice inter-metallic compounds with anti-structure defects. *Intermetallics* **1995**, *3*, 233–242. [[CrossRef](#)]
15. Tokuda, K.; Maki, J.; Goto, Y.; Mitsunobu, T. Coated Steel Product: United States. U.S. Patent 2019/0390303 A1, 26 December 2019.
16. Saito, M.; Goto, Y.; Ishizuka, K. Plated Steel Material: European. EP Patent 4 060 075 A1, 21 September 2022.

**Disclaimer/Publisher's Note:** The statements, opinions and data contained in all publications are solely those of the individual author(s) and contributor(s) and not of MDPI and/or the editor(s). MDPI and/or the editor(s) disclaim responsibility for any injury to people or property resulting from any ideas, methods, instructions or products referred to in the content.